Valve-Regulated Lead-Acid Batteries with a Extra Long Cycle Life for Power Storage System

(English translation of original Japanese paper TR15 published by Hitachi in 2005)

Hitachi developed a new design VRLA (Valve-Regulated Lead-Acid) Battery LL-S Series with long cycle life for power storage system to meet the increasing utilization of renewable energy and time shift of off-peak electric energy. The cycle life of this new battery is much improved by the adoption of the specifications as follows. ① positive plates with grid of high corrosion resistance alloy, designed to reduce deformation with adoption of high density active material, ② negative plates using new carbon for increasing charge performance, ③ new metal frame structure for decreasing of temperature rise and dispersion of cell temperature as used in a battery bank. It has excellent characteristic on cycle life performance of 4,500 cycles and charge-discharge efficiency of 87%. In demonstration test by running for over 2 and half years, it is confirmed that no problems were observed and that this battery is fit for purpose.

Contents

Development of Extra Long Life Valve-Regulated Lead-Acid-Batteries (VRLA-Batteries) for cyclical application Hitachi Type LL-S

1. Introduction

During recent years environmental issues such as the perceived global warming are pursued with greater attentiveness. By the Kyoto Protocol, that was passed at the conference of the Contracting States of the United Nations Framework Convention (COP3), climate reduction targets have been set to reduce emission greenhouse gas such as CO_2. Therefore different specific measures are still to be implemented.

While energy efficiency enhancement is still propelled by the Japanese industry, the personal electricity consumption still increases. Therefore the overall power usage is inclined to rise further. To reach the emission targets radical measures are required. Besides the reduction of the entire electricity consumption it is also important to deal with the network load compensation between day and night, as the power usage is concentrated during daytime. If the superfluous energy would be accumulated (stored up) by electricity storage systems and used during the day, the power production volume (output) could be reduced. That would be a significant tool for the load compensation as well as for the reduction of the CO_2 emission. Consumers would profit from the lesser electricity costs as the lower price night current would be used for the peak load reduction.

Various electricity storage systems are currently developed whereby different batteries are utilized, such as Lead-Acid-Batteries, Sodium-Sulfur-Storage-Batteries, Redox-Flow-Batteries and Lithium-Ion-Batteries. Different questions still have to be dealt with, such as durability, costs and space required for installation.

The Valve-Regulated Lead-Acid-Batteries have its advantage in regards to low costs and easy handling, reliability and security. Therefore the developmental word for durable batteries and electricity storage systems has been propelled to attain practical application. Also another field of application is lately pursued intensively, where batteries come into operation combined with photo-voltaic-systems or wind power plants. A great need of durable VRLA-Batteries for cyclical usage is expected in the future.

Hitachi had already developed the VRLA-Battery Type LL with a durability of 3000 cycles. They are continuously working on the durability increase aiming to reach the durability of 4500 cycles. This project was approved as a Government funded project between 2001 to 2003 by the New Energy and Industrial Technology Development Organization (NEDO). The following will report on this developmental work.

2. Developmental Targets

The following goals were set:

(1) A single cell battery with high capacity 2V-1000Ah, 2V-1500Ah
(2) Durability: 4500 cycles (70% discharge depth, 25°C)
(3) Charging Efficiency Factor: 87%

3. Lifetime increase of the Battery

The structure of the VRLA batteries is shown in **Figure 1**

図１　制御弁式据置鉛蓄電池の構造
Fig.1 Internal Structure of Stationary VRLA Battery.

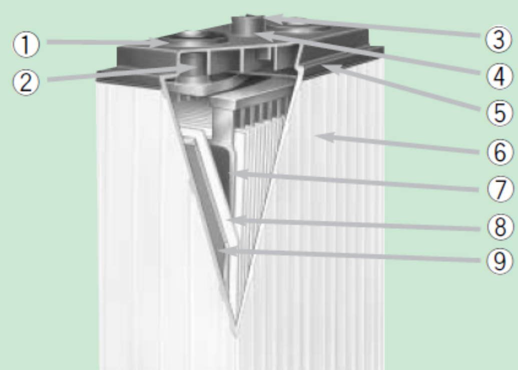

No.	部品名
①	端子
②	極柱
③	安全弁
④	防爆防まつ装置
⑤	蓋
⑥	電槽
⑦	正極板
⑧	リテーナ（セパレータ）
⑨	負極板

1) Terminal 2) Terminal bush/insert 3) Safety Valve, 4) Explosion- and Shatter-Protection,
5) Cover 6) Shell, 7) Positive electrode 8) Retainer (Separator), 9) Negative electrode

Inside the shell there are electrode groups consisting of negative electrodes and separators. The fiberglass-fleece separators are called "Retainers". Diluted sulfuric acid serves as electrolyte and is held by the electrode groups. The pole grid consists of lead alloy grates and are furnished with porous active mass (lead dioxide with the positive electrode, lead sponge with the negative electrode.

Fixed lead batteries were mainly used as emergency generators or uninterrupted power supplies for stand-by-usage. Compared with this the already existing VRLA-Battery Type LL (with duration of 3000 cycles) is characterized by the following:

- High density positive active mass
- Optimized additive for negative electrodes
- Horizontal position of battery (terminals to the side) and the appropriate retainer
- Optimized charging method

Through this it was possible to increase the duration to 3000 cycles. In **Figure 2** the result of the cycle endurance test is shown and in **Table 1** the result of the teardown study of the batteries that had reached the end of its durability is shown.

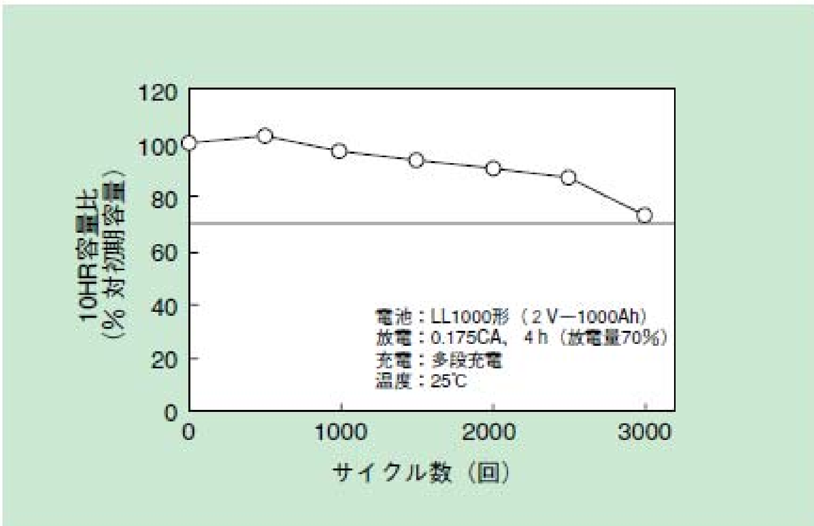

図2　LL形電池（3000サイクル寿命）の寿命試験結果
Fig.2 Result of Cycle Test of LL Type Battery (2V-1000Ah, 3000 Cycle Life) at 25℃.

Cycle test for VRLA-Battery Type LL (with duration of 3000 cycles)
Vertical axis: Capacity (10HR) in relation to its original condition (%)
Horizontal axis: cycle number

Battery: Type LL-1000 (2V-1000Ah)
Discharge: 0.175CA, 4h (discharged amount of electricity 70%)
Charging: Multi-stage charging
Temperature: 25°C

Table 1 Result of Battery Disassemble Survey.

項目		評価	
正極	格子腐食	×	格子腐食・変形が大きい
	活物質泥状化	×	泥状化あり
負極	サルフェーション	×	硫酸鉛の蓄積あり
電解液	成層化	○	問題なし
	減液	○	問題なし
短絡		○	発生なし

After the batteries had reached their durability with 3000 cycles in the cycle test, they were dismantled and examined. This showed corrosion and deformation of the positive gratings, the non-retention of some of the positive active mass and the sulfation of the negative panel was noticed. Both of this exerts influence of the durability of batteries.

The following reports on the implemented improvement actions to increase the cycle cohesiveness.

3.1 Positive Gratings

To order to increase the durability of the positive gratings it is essential to prevent corrosion and the deformation of the gratings that goes along with it. Therefore Pb-Ca-Sn-alloyage with the optimized Ca- and Sn-dosage was used as grating material. This alloyage is corrosion resistant and features even corrosion which leads to only allowing very little deformation.

To prevent the deformation that goes along with the corrosion also a simulation for the corrosion and deformation of the gratings was performed and the grating-design was taken from it.

In reality the gratings deformation caused by corrosion occurs as a result of expansion of the surface layer of the gratings. In order to display this phenomenon as realistic as possible, the shaping was approached like this: First the gratings were warmed externally and according to the internal thermal conduction a heat distribution of the gratings was created. From each respective temperature increase the expansion quantity was calculated. At the shaping, this was then regarded as the volumetric expansion caused by corrosion. The temperature distribution of the gratings of the simulation analysis is shown in **Figure 3**. In this simulation, different cross-sectional areas, cross-sectional designs and proportions of the thick and thin gratings elements were modeled. One example is shown in **Figure 4**. Based on the simulation results the gratings design was determined to only allow a minimum weight increase which creates less deformation in regards to the previous battery.

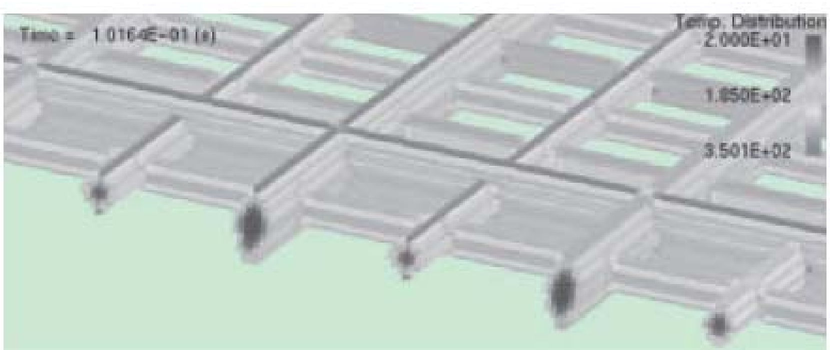

図3　解析時の格子の温度分布
Fig.3 Temperature Distribution in Simulation Model of the Grid.

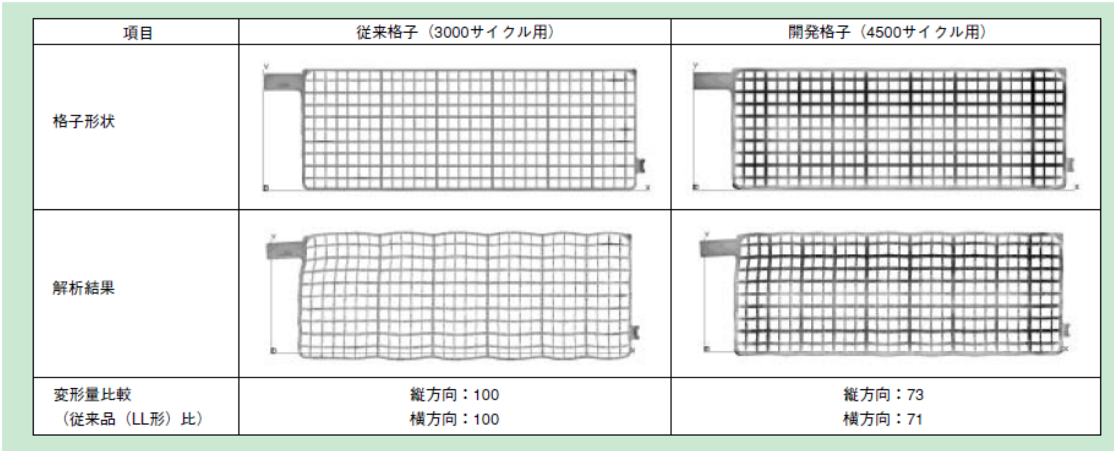

図 4　正極格子腐食変形シミュレーション結果の一例
Fig.4 The Illustration of Simulated Corrosion Deformation in Positive Grid.

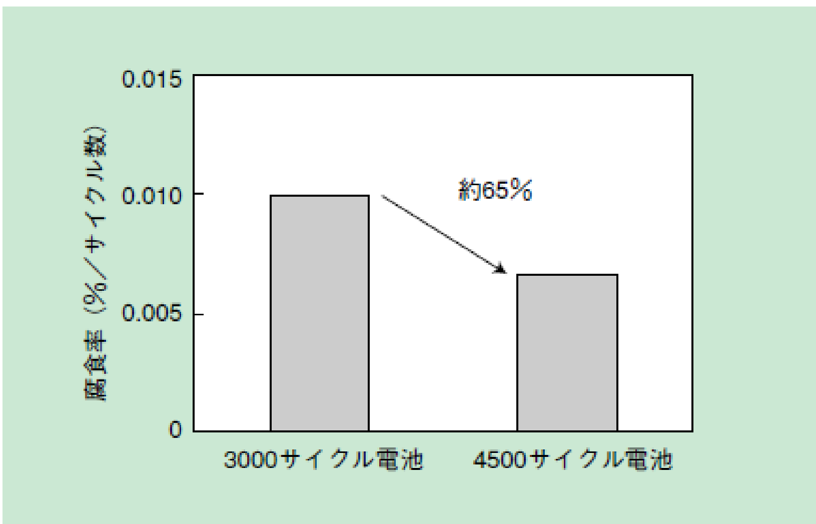

図 5　正極格子腐食量の比較
Fig.5 Comparison of Corrosion Rate of Positive Grids.

The comparison of the gratings corrosion amount at the cycle test between previous batteries (durability: 3000 cycles) to the new battery (durability: 4500 cycles) is shown in **Figure 5**. The corrosion amount of the new battery was 65% in relation to the previous ones. The durability of the gratings is magnified by 1.5. Thus this grating is able to provide the durability of 4500 cycles.

The positive mass changes its volume according to the charging- and discharging process. The connection between particles of the active mass loosens and the conductive network is destroyed (softening and sedimentation of the active mass). Consequently the capacity decreases. To prevent softening and sedimentation, it is sensible to increase the density of the active mass to ensure as many junctures as possible between the particles, giving it more stability.
To evaluate the active mass a cycle test was performed with a small test battery using a corrosion and deformation resistant energy collector as gratings with high

density active mass. The result is shown in **Figure 6**. This established that this active mass has an operational usage of over 4500 cycles.

As described above, a lightly deformed grating and a high density active mass resulted, ensuring the operation exceeding 4500 cycles with the positive grating.

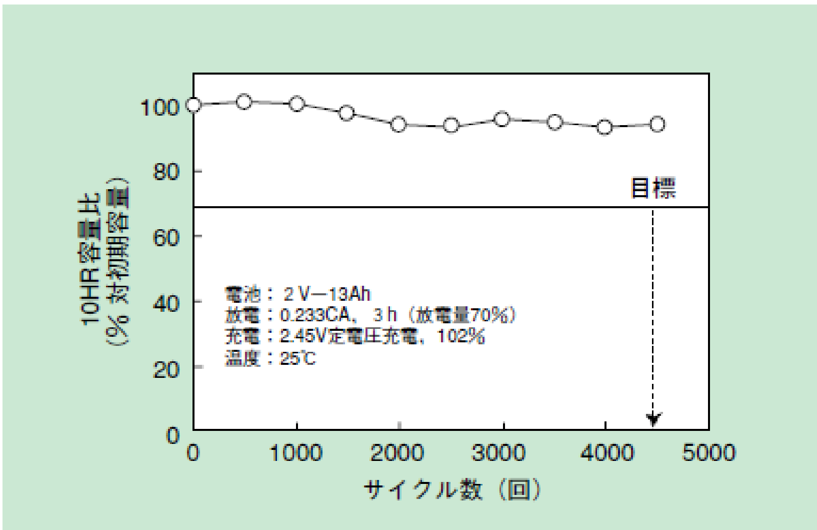

図6　試験用電池によるサイクル寿命試験結果
Fig.6　Results of Cycle Endurance Test by Test Cell.

Result / Conclusion of the cycle test with a trial battery

Vertical axis: Capacity (10 HR) in relation to its original condition (%)
Horizontal axis: Cycle amount

Battery: 2V-13Ah
Discharge: 0.233 CA, 3h (discharged amount of electricity 70%)
Charging: 2.45V constant voltage to 102%
Temperature: 25°C

3.2 Negative Gratings

In the charging and discharging process sulfation occurs of the negative mass. Through the increase of the particle size also the surface of the active mass decreases. Like the sulfation, this leads to a decrease of capacity. As a preventive action additives such as carbon, Lignin or Barium sulphate were added. The additives – depending on kind and amount – have a great influence on the discharge features, loading acceptance quality (absorption) and durability of the negative electrode.

It was already reported in the literature that carbon functions as a core of lead sulfate and is integrated into the lead sulfate. This is to increase the electrical conductivity of the lead sulfate surface. The surface of the carbon seems to enact a part in this. It is also known that finer-grained carbon and its increasing amount influences the charging degree. As the physical features of the carbon varies substantially depending on its type, the effects as additives for the negative active mass should also vary depending on the carbon types.

In order to detect different reactions of the carbon types in regards to the charging degree of the negative electrodes in good time, a comparative cycle test was performed with smaller trial batteries. Six carbon types were tested in cycles in which the batteries were discharged to 70% discharging depth and charged to 101% of the discharging amount under constant pressure. Respectively after 1000 cycles the lead sulfate amount of the negative electrode was determined. The result is shown in **Figure 7**. The lead sulfate amounts vary depending on the used carbon types: In relation to carbon type A, that was previously used, less lead sulfate was measured in types D and E. An improvement of the charging degree of the negative electrode was respectively noticed at type D and E.

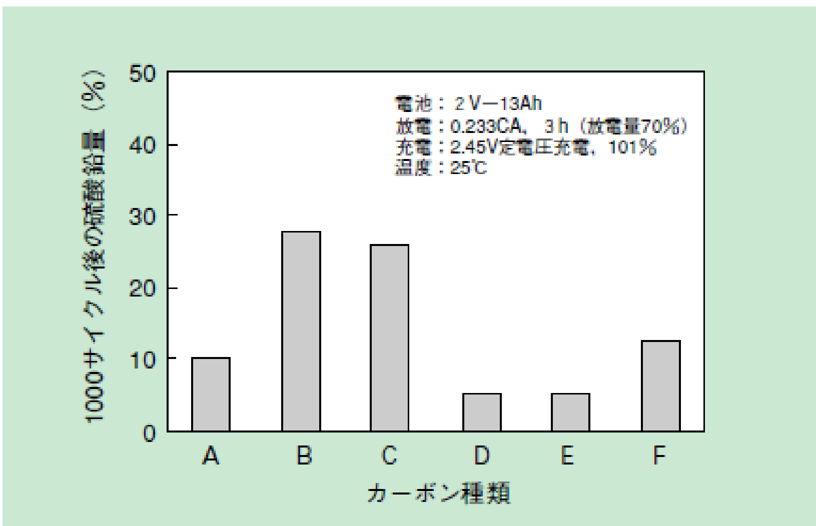

図７　カーボンの種類による硫酸鉛蓄積量の比較
Fig.7 Comparison of Amount of Lead Sulfate in Negative Active Material Using Different Carbon.

Vertical axis: amount of lead sulfate after 1000 cycles (%)
Horizontal axis: carbon types (A to F)

Battery: 2V – 13 Ah
Discharge: 0.233CA, 3h (discharge amount 70%)
Charging: 2.45V constant voltage to 101%
Temperature: 25°C

Physical features of the tested carbon types are shown in **Table 2**. No correlation could be detected between these features and the charging level of efficiency. Seemingly the amounts and styles of the surface functional groups of the carbon particle material are an issue. The mechanism of action of the carbon is still a matter of research at this time.

Table2　Comparison of Carbon Used for the Test.

試料	A（現行）	B	C	D	E	F
粒子径	1.0	0.1	0.5	1.0	1.0	短繊維
表面積	1.0	23.0	16.0	4.0	1.0	—
見かけ密度	1.0	1.7	1.5	2.0	6.0	5.0

4. Structure and Features of the newly developed battery

4.1 single cell battery

The specifications of the newly developed Batteries Type LL-S, with a durabilty of 4500 cycles, are shown in **Table 3.** The following articles that are mentioned in position “Battery structure and Working Condition” was taken from the already applied technology of Battery Type LL:

- Installation of the Battery in lateral position (polarity gratings in horizontal direction)
- Appropriate Retainer for lateral position
- Charging Control System through current quantity control

Table 3　Specifications of the newly developed Battery Type LL-S

表３　制御弁式鉛蓄電池LL-S形の内容と目的
Table 3　Content and Purpose of the Developed Battery.

項目	内容	目的
正極	高耐食性合金（Pb−Ca−Sn）格子 格子の腐食変形が小さいデザイン	正極格子の腐食変形抑制
	高密度・高強度活物質 高加圧による活物質保持	活物質泥状化・崩壊抑制
負極	添加剤の改良 リグニン カーボン	充電受入性向上・サルフェーション抑制 充放電効率向上 充電電気量抑制による正極格子腐食抑制
電池構成 使用条件	電池の横置き設置（極板水平方向） 横置きに適したリテーナ採用 添加剤の使用 封口剤・ブッシング形状変更	成層化抑制 耐漏液信頼性向上
	電気量管理による充放電制御	過充電制御による正極格子腐食抑制 電力効率向上

表４　開発電池（LL-S形）と従来電池（LL形）の比較
Table 4　Comparison of Specifications with Developed Batteries and the Before.

型式		電圧（V）	定格容量（Ah）	外形寸法（mm）			重量（約kg）	期待寿命※（サイクル）
				高さ	長さ	幅		
開発電池	LL1000−S	2	1000	507	303	172	72	4500
	LL1500−S	2	1500	507	437	172	106	4500
従来電池	LL1000	2	1000	507	303	172	67	3000
	LL1500	2	1500	507	437	172	98	3000

※：DOD70%，25℃，推奨充電条件

表５　組電池における電池温度上昇と電池間温度ばらつき抑制に関する検討結果
Table 5　Results for Decrease of Temperature Rise and Dispersion of Set Battery.

項目	結果	期待効果	
		温度上昇	温度ばらつき
電池間隔	20mm以上必要	約４℃低下	約５℃減少
送風	20cm／sec以上必要	約３℃低下	約３℃減少
充電条件（第１段目充電電力）	充電電力値が小さい程効果大	約３℃低下	約２℃減少
放電条件（放電深度）	浅い程効果大	約３℃低下	約２℃減少

In **Table 4** the specifications of the newly developed batteries are shown in relation to the previous ones. The exterior view of the new batteries (LL 1000-S and LL1500-S) is shown in **Figure 8**. The new batteries have the same exterior measurements as the previous ones with 3000 cycles. The weight has increased by 8% and the durability has increased 1.5 times to 4500 cycles.

Polypropylene, which marks durability stability against chemical and resists humidity, was used for the shell. The terminals were applied as “Terminal inserts”. The lead alloy straps (busbar) and the terminal inserts were connected by TiG welding. Epoxy resin was used as sealing compound for the cover and shell. This construction ensures no electrolyte leakage.

図８　開発電池の外観写真
Fig.8　Appearance of Developed Batteries.

図12　LL15000—S組電池の一例
Fig.12　Set of LL1500-S Battery. (12 Pieces)

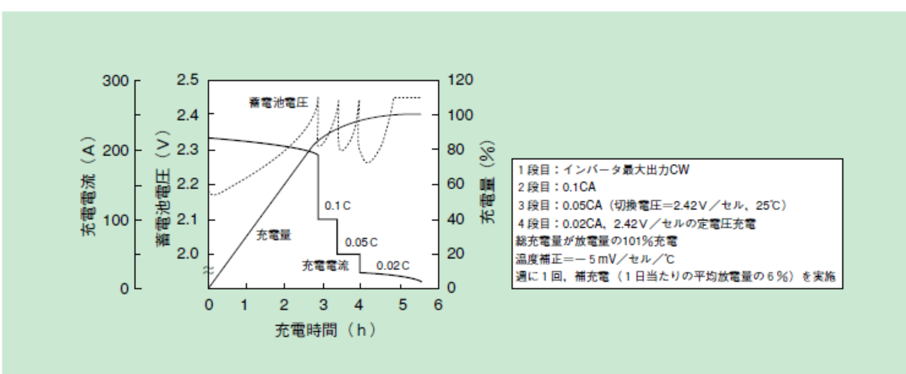

図９　推奨充電方法
Fig.9　Recommendation Charging Pattern.

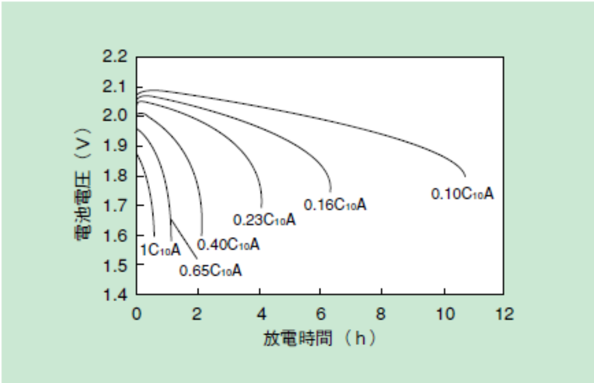

図10　LL1000—S形電池の各率放電特性（25℃）
Fig.10　Discharge Characteristics of LL1000-S at 25℃.

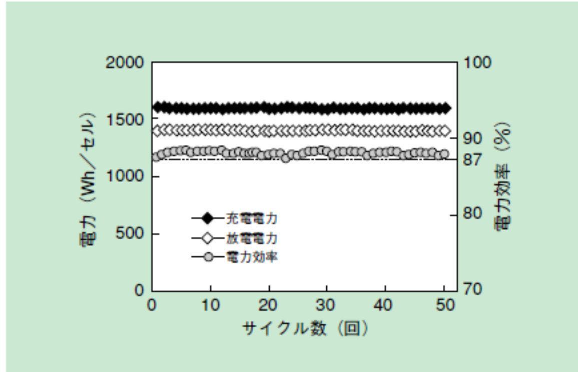

図11　LL1000—S形電池の充放電サイクル時の電力効率
Fig.11　Power Efficiency During Cycle Test at 25℃.

The recommended charging method is shown in **Figure 9**. This is a multi-stage-charging: After reaching the predefined 2.43V/cell the charging current is reduced progressively. In order to prevent overcharging, the charging current quantity is limited.

Figure 9

1. Level: maximum capacity of Inverters CW
2. Level: 0.1CA
3. Level: 0.05CA (Switching at 2.24V/Cell Voltage at 25°C)
4. Level: 0.02CA, Constant Voltage Charging with 2.42V/Cell)

Total Charging Amount: 101% of the Discharge Current Amount
Temperature compensation: -5mV/Cell/°C)
Carry out one auxiliary charging per week (65 of the average quantity).

In **Figure 10** the discharging-characteristics of the newly developed Battery (Type LL 1000) is shown with various discharging methods at 25°C. The discharge efficiency is similar to the previous Battery Type LL.

Figure 10 Discharge Characteristic of the newly developed battery (Type LL 1000-S) at various discharge rates at 25°C

Vertical axis: Battery voltage (V)
Horizontal axis: Charging Time (h)

After discharging to 70% discharging depth a cycles test was carried out according to the recommended charging method (see **Figure 11**). The performance efficiency of the Battery Type LL 1000-S was approx. 87% (roundtrip)

Figure 11 Performance Efficiency of Battery Type LL 1000-S in a cycle test at 25°C

Vertical axis left: Performance (Wh/Cell)

Vertical axis right: Performance Rate (%)
Horizontal axis: cycle number

Lines from above: - Charging Current
- Discharging Current
- Performance Rate

4.2 Battery Banks

Many batteries are needed for electricity storage systems. They are joined together in a metal frame and put into service as a modular unit. An example of such battery-banks (Type LL1500AS8) is shown in **Figure 12.** Temperature deviations occur between the different batteries depending on their position within the battery-bank. The corrosion capacity of the positive gratings also increases as temperature rises. **Figure 13** shows the proportion between the temperature at the cycle test and the corrosion capacity of the positive gratings. Therefore it is important to reduce an increase of temperature and to minimize the temperature difference between the individual batteries in application of batteries as a battery-bank.

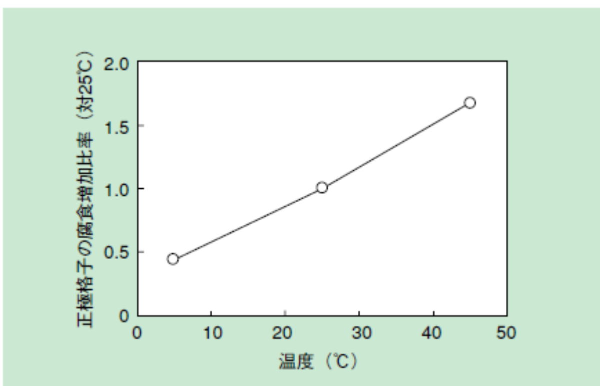

図13 サイクル試験時の温度と正極格子腐食量の関係
Fig.13 Relationship Between Temperature and Corrosion Rate of Positive Grid.

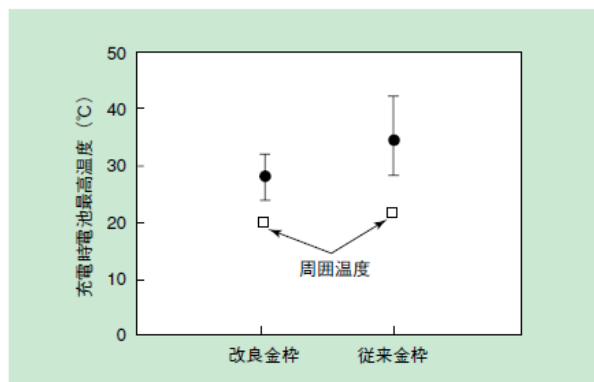

図14 金枠の効果
Fig.14 Effect of Metal Flame Structure .

Figure 13 Relations between the temperature at the cycle test and the corrosion capacity of the positive gratings

Vertical axis: Expansion rate of the corrosion of the positive gratings (in relation to the corrosion at 25°C) (%)

Horizontal axis: Temperature (°C)

To prevent temperature rising of batteries and temperature deviations between the individual batteries during cycling of the battery bank, a simulation analysis has been performed. The results have been compared with the real measurement data. During the simulation the thermal conduction analysis and the heat convection analysis have been combined. During the actual measurements recreated metal frames were used for the battery-banks. The results are shown in **Table 5**. Hence it follows, that the consecutive measures are effective to prevent temperature rise of the batteries and temperature deviations amongst the batteries during cycling of the battery-banks:

- design the structure of the metal frame ensuring spacing between the batteries.
- airing/venting the batteries.
- reduction of charging current in the first stage with multi-stage charging (shown in Figure 9).
- a lesser discharge-depth

As the charging current and the discharge-depth depend on the operating conditions, an improved metal frame was implemented. The frame structure was changed to ensure spacing between the batteries. Thus the batteries were aired/vented. The results of these two schemes indicate that the temperature rise during cycling can be reduced by approx. 7°C and that temperature deviations between the batteries could be reduced by approx. 8°C each time.

表５　組電池における電池温度上昇と電池間温度ばらつき抑制に関する検討結果
Table 5 Results for Decrease of Temperature Rise and Dispersion of Set Battery.

項目	結果	期待効果	
		温度上昇	温度ばらつき
電池間隔	20mm以上必要	約４℃低下	約５℃減少
送風	20cm／sec以上必要	約３℃低下	約３℃減少
充電条件（第１段目充電電力）	充電電力値が小さい程効果大	約３℃低下	約２℃減少
放電条件（放電深度）	浅い程効果大	約３℃低下	約２℃減少

A cycle test of the 1500Ah-battery-bank was performed while using the optimized metal frames to conduct an equation. Thus four batteries were placed into one metal frame. This module was stacked up in three stages, so that one battery-bank contained 12 batteries. The comparative result is shown in **Figure 14**. Through the usage of the optimized metal frames the temperature rise of the batteries each could be reduced by an average of approx. 6°C and the temperature deviations between the batteries by approx. 4°C. Further improvement of the results is expected, while performing an optimized of the airflow between the batteries.

Figure 14 Effect of the metal frame improvement

Vertical axis: Maximum temperature of the batteries at charging (°C)
Horizontal axis left: With the optimized metal frame
Horizontal axis right: With the conventional metal frame
(within Figure): Ambient temperature

5. Trial test in practical application

A trial test with three electricity storage systems was performed at the Hitachi factory They were connected to the grid and operated in “Peak-Shift” Mode. The survey of these storage systems is shown in **Table 6**. Unit 1 and 2 are equipped with a maximum discharge capacity of 100kW and unit 3 of 400kW.

表６　実用試験中の電力貯蔵システムの構成
Table 6 Outline of Power Storage System for Demonstration Test.

項目		１号機（図15）	２号機	３号機
システム容量		100kW	100kW	400kW
方式		系統連系双方向コンバータ		
使用電池		2000Ah電池 （1000Ah電池－２並列） 144セル直列	1500Ah電池 192セル直列	4000Ah電池 （1500Ah－1500Ah－ 1000Ah電池－３並列） 240セル直列
稼働開始		2002年４月	2002年11月	2003年11月
稼働条件	放電	50kW，８h（月～土）	50kW，８h（月～土）	150kW，８h（月～土）
	充電	推奨充電方式（多段充電）101%充電（月～土，22：00～8：00）		
	補充電	６%（日曜）		

Unit 1, which has operated the longest, is shown in **Figure 15**. **Figure 16** shows the voltage at the end of discharge for unit 1. During the continuous operation over 2 years and 6 months, neither any drop-off, nor deviation in battery voltage increase could be established. The same applies to units 2 and 3.
To this day, all three units provide very good results as a complete system. Thus establishing the application efficiency/serviceability of the batteries in application as electricity storage systems.

100kWシステム　　電池（2000Ah－144セル）

図15　電力貯蔵システム１号機（100kW）
Fig.15 Power Storage System for Demonstration Test.

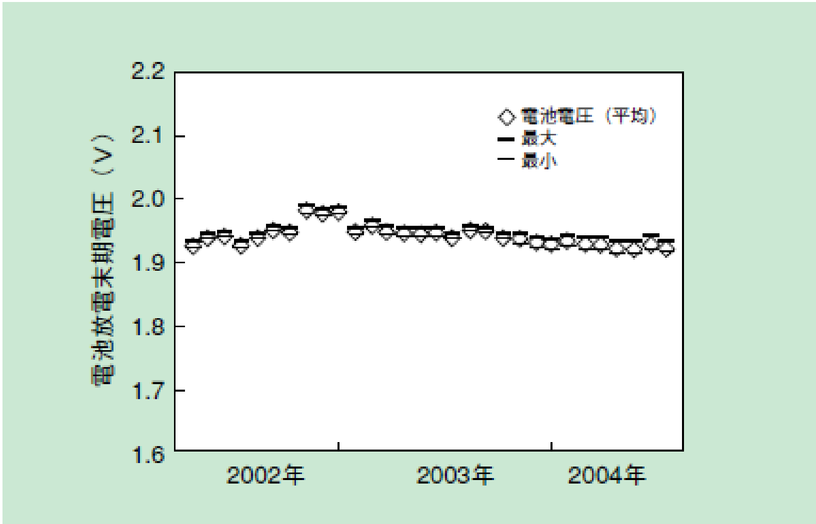

図16　システム試験における電池の放電末期電圧の推移
Fig.16 Change in Discharge End Voltage of Batteries During the System Test.

Figure 15 Electricity storage systems (Unit 1)
Figure left: 1000kW-System
Figure right: Batteries (2000Ah, 144 Cells)

Figure 16 Development of electric voltage at the end of discharging at the system test (Unit 1)
Vertical axis: Battery voltage at the end of discharge (V)
Horizontal axis: Years 2002 – 2004

6. Summary/Abstract

The long life valve regulated lead-acid-batteries (VRLA-Batteries) for cyclical application Type LL1500AS2 and LL1000AS2 were developed for the operation as electricity storage systems:

(1) Life of 4500 cycles (70% discharge-depth at 25 °C) could be established with:

- corrosion free alloy gratings, which are capable of minimizing deformations caused by corrosion.
- High density positive active mass.
- Improved charging capacity ability of negative electrodes by modification of carbon additives
- Increased reliability by improving the sealing area.

(2) A battery-bank metal frame, that is able to reduce temperature rising of the batteries and temperature deviations between batteries, was developed.

(4) By the trial test of practical operation as an electricity storage system of 2 years and 6 month it was established that a successful operation is ensured.

(7. Acknowledgement to NEDO for your support)